Available online at www.sciencedirect.com
SCIENCE DIRECT®
Journal of Chromatography A, 1098 (2005) 82–94
JOURNAL OF CHROMATOGRAPHY A
www.elsevier.com/locate/chroma

Effect of the endcapping of reversed-phase high-performance liquid chromatography adsorbents on the adsorption isotherm

Fabrice Gritti[a,b], Georges Guiochon[a,b,*]

[a] *Department of Chemistry, University of Tennessee, Knoxville, TN 37996-1600, USA*
[b] *Division of Chemical Sciences, Oak Ridge National Laboratory, Oak Ridge, TN 37831-6120, USA*

Received 5 November 2004; received in revised form 23 December 2004; accepted 17 August 2005
Available online 19 September 2005

Abstract

The retention mechanisms of *n*-propylbenzoate, 4-*tert*-butylphenol, and caffeine on the endcapped Symmetry-C_{18} and the non-endcapped Resolve-C_{18} are compared. The adsorption isotherms were measured by frontal analysis (FA), using as the mobile phase mixtures of methanol or acetonitrile and water of various compositions. The isotherm data were modeled and the adsorption energy distributions calculated. The surface heterogeneity increases faster with decreasing methanol concentration on the non-endcapped than on the endcapped adsorbent. For instance, for methanol concentrations exceeding 30% (v/v), the adsorption of caffeine is accounted for by assuming three and two different types of adsorption sites on Resolve-C_{18} and Symmetry-C_{18}, respectively. This is explained by the effect of the mobile phase composition on the structure of the C_{18}-bonded layer. The bare surface of bonded silica appears more accessible to solute molecules at high water contents in the mobile phase. On the other hand, replacing methanol by a stronger organic modifier like acetonitrile dampens the differences between non-endcapped and endcapped stationary phase and decreases the degree of surface heterogeneity of the adsorbent. For instance, at acetonitrile concentrations exceeding 20%, the surface appears nearly homogeneous for the adsorption of caffeine.

Keywords: Adsorption equilibrium; Frontal analysis; Overloaded band profiles; Column heterogeneity; Affinity energy distribution; End-capping; Resolve-C_{18}; Symmetry-C_{18}; 4-*tert*-Butylphenol; Caffeine; Propylbenzoate

1. Introduction

Now, most routine analytical separations in the pharmaceutical, biomedical, and environmental industries use reversed-phase liquid chromatography (RPLC) as the most convenient technique. A large number of RPLC columns are commercially available, exhibiting a large variety of physico-chemical properties, e.g., the length of their bonded ligand (C_4, C_8, C_{18}, C_{30}, ...), the ligand surface density, the chemical nature of the underlying solid adsorbent (silica, crossed linked polymers, hybrid materials, ...), the surface area of the material and its pore size distribution. Another very important characteristic of RPLC columns is whether the adsorbent surface is endcapped, e.g., whether part of the residual silanols that remain on the surface after completion of the ligand bonding process has been eliminated by a step of trimethylsilylation. Endcapping is a well known technique that significantly reduces the peak asymmetry of basic solutes by limiting the possibilities of strong interactions between amine and silanol functions. Much work was done to demonstrate the effects of acidic silanol groups on the retention, peak shape, and column selectivity of basic compounds under analytical conditions [1–3]. Some models applicable in linear chromatography were also derived to combine the contribution of the reversed-phase process and the contribution of the ion-exchange with surface silanol groups [4]. It was shown that experimental data measured on endcapped columns were consistent with a retention mechanism involving the interaction of a positively charged analyte with ionized silanols located either amidst the network of C_{18} chains (and so, not in direct contact with the mobile phase) or on the free silica surface in contact with the mobile phase.

A different approach was used recently to determine the retention mechanism of a positively charged compound on various silica-C_{18} stationary phases under various pH [5,6] and supporting salt conditions [7–9]. This study was not limited to concentrations in the analytical range but encompassed the largest concentration range allowed by the analyte solubility in

* Corresponding author. Tel.: +1 865 974 0733; fax: +1 865 974 2667.
E-mail address: guiochon@utk.edu (G. Guiochon).

0021-9673/$ – see front matter © 2005 Elsevier B.V. All rights reserved.
doi:10.1016/j.chroma.2005.08.045

the mobile phase. This approach allows the determination of the column loadability. It also gives insights on the degree of heterogeneity of the surface without requiring any model assumptions. The acquisition of isotherm data by frontal analysis and the treatment of these data to derive the adsorption energy distribution (AED) confirmed the existence of two independent sites in this case. Approximately 99% of the surface was covered with low adsorption energy sites, corresponding to the hydrophobic ligand, the remaining 1% were attributed to high adsorption energy sites that could be consistent with an ion-exchange mechanism.

In a separate study, the adsorption properties of a neutral and a mildly polar compound (phenol and caffeine) on a non-endcapped and an endcapped materials, Resolve-C_{18} and Xterra-C_{18}, respectively, were compared [10]. It was found that the retention mechanism of phenol is exactly the same whether the column is endcapped or not. The presence of free silanol groups did not influence significantly the adsorption of the neutral compound phenol. However, we found for caffeine an additional type of high-energy adsorption sites on Resolve-C_{18} while no equivalent type of sites was found on the endcapped Xterra-C_{18}, suggesting that these new sites were due to different hydrophobic environment in the C_{18}-layer structure of the Resolve-C_{18} but not to specific interactions with any silanol groups. This result is not really surprising since these two compounds are neutral and are almost not retained on the neat Resolve silica with the same mobile phase as used then (methanol/water, 70/30, v/v).

The generality of this initial result must be investigated by making similar measurements under different conditions, for example, with less polar compounds, using higher methanol concentrations. It is well known that the mobile phase composition plays a large role on the structure of the C_{18}-bonded layer and that some differences in this structure may be encountered between non-endcapped and endcapped adsorbents. The goal of this work consists in investigating the possible effect of the presence or absence of column end-capping on the isotherm parameters.

2. Theory

The adsorption isotherm data were acquired by frontal analysis. Details on this method are given elsewhere [11–14]. The determination of the adsorption energy distribution (relationship between the number of sites and their adsorption energy) was made by the expectation–maximization method, described previously [15,16]. The local isotherm assumed for homogeneous sites was either the Langmuir isotherm (for convex upward isotherm) or the Brunauer–Emmet–Teller (BET) isotherm (for S-shaped isotherm) [17]. The modeling of the overloaded band profiles was performed by using the equilibrium-dispersive model of chromatography. Details of this model were given in earlier publications [11,10].

2.1. Models of isotherm

The adsorption isotherm models used to account for the data obtained for caffeine, 4-*tert*-butylphenol and propylbenzoate were built using two simple models, the Langmuir and the BET models. For the first two compounds, we used the simple addition of several Langmuir models: the resulting overall adsorption models are called the Bi-, Tri- or Quadri-Langmuir isotherm depending on whether the surface of the adsorbent is assumed to be paved with two, three, or four different types of homogeneous chemical domains which behave independently. The corresponding models are the addition of two, three or four independent local Langmuir isotherms. Thus, we obtain the Bi-Langmuir isotherm model:

$$q^* = q_{s,1}\frac{b_1 C}{1+b_1 C} + q_{s,2}\frac{b_2 C}{1+b_2 C} \tag{3}$$

the Tri-Langmuir isotherm model:

$$q^* = q_{s,1}\frac{b_1 C}{1+b_1 C} + q_{s,2}\frac{b_2 C}{1+b_2 C} + q_{s,3}\frac{b_3 C}{1+b_3 C} \tag{4}$$

and the Quadri-Langmuir isotherm model:

$$q^* = q_{s,1}\frac{b_1 C}{1+b_1 C} + q_{s,2}\frac{b_2 C}{1+b_2 C} + q_{s,3}\frac{b_3 C}{1+b_3 C} + q_{s,4}\frac{b_4 C}{1+b_4 C} \tag{5}$$

These models have one, two, three, or four saturation capacities, respectively, $q_{s,1}$, $q_{s,2}$, $q_{s,3}$, and $q_{s,4}$, that are related to the surface area occupied by each one of the different types of sites found on the surface. The equilibrium constants b_1, b_2, b_3, and b_4 are associated with the adsorption energies $\epsilon_{a,1}$, $\epsilon_{a,2}$, $\epsilon_{a,3}$, and $\epsilon_{a,4}$, through the following equation [17]:

$$b_i = b_0 e^{(\epsilon_{a,i})/RT} \tag{6}$$

where $\epsilon_{a,i}$ is the energy of adsorption, R the universal ideal gas constant, T the absolute temperature and b_0 is a preexponential factor that could be derived from the molecular partition functions in both the bulk and the adsorbed phases. b_0 is often considered independent of the adsorption energy $\epsilon_{a,i}$ [17]. The adsorption energy distribution (AED) functions, $F(\epsilon)$, of the Bi-Langmuir, Tri-Langmuir and Quadri-Langmuir are the sums of two, three or four Dirac functions, respectively.

On the other hand, the BET isotherm model accounts well for the adsorption of the alkylbenzoates, as reported elsewhere [18–21]. This isotherm model is:

$$q^* = q_s\frac{b_S C}{(1-b_L C)(1-b_L C+b_S C)} \tag{4}$$

where q_s is the monolayer saturation capacity of the adsorbent, b_S the equilibrium constant for surface adsorption–desorption over the free surface of the adsorbent and b_L is the equilibrium constant for surface adsorption–desorption over a layer of adsorbate molecules. This model accounts for local adsorption [17].

3. Experimental

3.1. Chemicals

The mobile phases used in this work were mixtures of methanol and water (30:70, 60:40, 65:35, v/v) or acetonitrile

Table 1
Physico-chemical properties of the C_{18}-bonded packed Xterra column (150 mm × 3.9 mm)

Column	Resolve-C_{18}	Symmetry-C_{18}
Particle shape	Spherical	Spherical
Particle size (μm)	5	5
Pore size[a] (Å)	90	86
Pore volume[a] (mL/g)	0.50	0.90
Surface area[a] (m^2/g)	200	346
Total carbon (%)	10.2	19.6
Surface coverage (μmol/m^2)	2.45	3.18
Endcapping	No	Yes

[a] Data for the packings before derivatization.

and water (20:80), all HPLC grade, purchased from Fisher Scientific (Fair Lawn, NJ, USA). The solvents used to prepare the mobile phase were filtered before use on an SFCA filter membrane, 0.2 μm pore size (Suwannee, GA, USA). Thiourea was chosen to measure the column hold-up volume. Thiourea, 4-*tert*-butylphenol, propylbenzoate and caffeine were all obtained from Aldrich (Milwaukee, WI, USA).

3.2. Columns

Two columns were used in this study, packed with the end-capped Symmetry-C_{18} and the non-endcapped Resolve-C_{18}. They had been given by the manufacturer (Waters Corporation, Milford, MA, USA). Both columns have the same size 150 mm × 3.9 mm. The main characteristics of the bare porous silica and of the packing material used are summarized in Table 1. The hold-up times of these columns were derived from the retention time of two consecutive thiourea injections and the corresponding porosities measured as a function of the mobile phase composition are showed in Table 2.

3.3. Apparatus

The isotherm data were acquired using a Hewlett-Packard (Palo Alto, CA, USA) HP 1090 liquid chromatograph. This instrument includes a multi-solvent delivery system (tank volumes, 1 L each), an auto-sampler with a 250 μL sample loop, a diode-array UV- detector, a column thermostat and a data station. Compressed nitrogen and helium bottles (National Welders, Charlotte, NC, USA) are connected to the instrument to allow the continuous operations of the pump, the auto-sampler, and the solvent sparging. The extra-column volumes are 0.068 and 0.90 mL as measured from the auto-sampler and from the pump system, respectively, to the column inlet. All the retention data were corrected for this contribution. The flow-rate accuracy was controlled by pumping the pure mobile phase at 23 °C and 1 mL/min during 50 min, from each pump head, successively, into a volumetric glass of 50 mL. The relative error was less than 0.4%, so that we can estimate the long-term accuracy of the flow-rate at 4 μL/min at flow rates around 1 mL/min. All the measurements were carried out at a constant temperature of 23 °C, fixed by the laboratory air-conditioner. The daily variation of the ambient temperature never exceeded ±1 °C.

Table 2
Total column porosities of the Resolve-C_{18} and Symmetry-C_{18} columns as a function of the mobile phase used

Mobile phases	Resolve-C_{18}	Symmetry-C_{18}
MeOH/H_2O, 65/35 (v/v)	0.5998	0.5849
MeOH/H_2O, 60/40 (v/v)	0.6014	0.5790
MeOH/H_2O, 30/70 (v/v)	0.6240	0.5921
ACN/H_2O, 20/80 (v/v)	0.6155	0.5759

3.4. Measurements of the adsorption isotherms by FA

The maximum concentration of caffeine used in the FA runs in the methanol:water (30/70, v/v) and acetonitrile:water (20/80, v/v) mixtures were fixed at 25 and 40 g/L, respectively. Those of 4-*tert*-butylphenol and propylbenzoate were 30 and 15 g/L in their respective mobile phase composition (methanol:water, 60/40 and 65/35 (v/v), respectively). Two master solutions were prepared (allowing the acquisition of a total of 31 data points, see procedure below), at 10 and 100% of the maximum concentration for the measurement of the adsorption data of caffeine in order accurately to measure the adsorption data from the lowest concentrations (where the isotherm is linear) to the maximum concentration (large enough to approach the column saturation capacity). Only one master solution was necessary for the adsorption measurement of 4-*tert*-butylphenol (18 data points) and propylbenzoate (17 data points).

One pump (A) of the HPLC instrument was used to deliver a stream of the pure mobile phase, the second pump (B and C for the 100 and the 10% solution, respectively), a stream of the sample solution. The concentration of the sample in the FA stream is determined by the concentration of the mother sample solution and the flow rate fractions delivered by the two pumps. All the breakthrough curves were recorded at a flow rate of 1 mL min^{-1}, with a sufficiently long time delay between each breakthrough curve to allow for the complete reequilibration of the column with the pure mobile phase. The injection time of the sample was fixed at 5 min for all FA steps in order to reach a stable plateau at the column outlet. To avoid recording any UV-absorbance signal larger than 2500 mAU and the lose accuracy for the corresponding signal noise at the highest concentrations while, in the same time, keeping a large enough signal for the lowest concentrations, the detector signal was detected at 297 nm (10% solution) and 305 nm (100% solution) for caffeine. A single UV wavelength was used to record the breakthrough curves of *tert*-butylphenol and propylbenzoate at 295 and 293 nm, respectively. In each case, the detector response was calibrated accordingly by using the UV absorbance at the plateau observed on the breakthrough curves.

4. Results and discussion

4.1. Adsorption of propylbenzoate on Resolve-C_{18} and Symmetry-C_{18} (MeOH/H_2O, 65/35, v/v)

The amount of propylbenzoate adsorbed per unit volume of each adsorbent is plotted versus the mobile phase concentration in Fig. 1. A non-conventional S-shaped isotherm is observed, that is initially convex upward at low concentrations, experiences

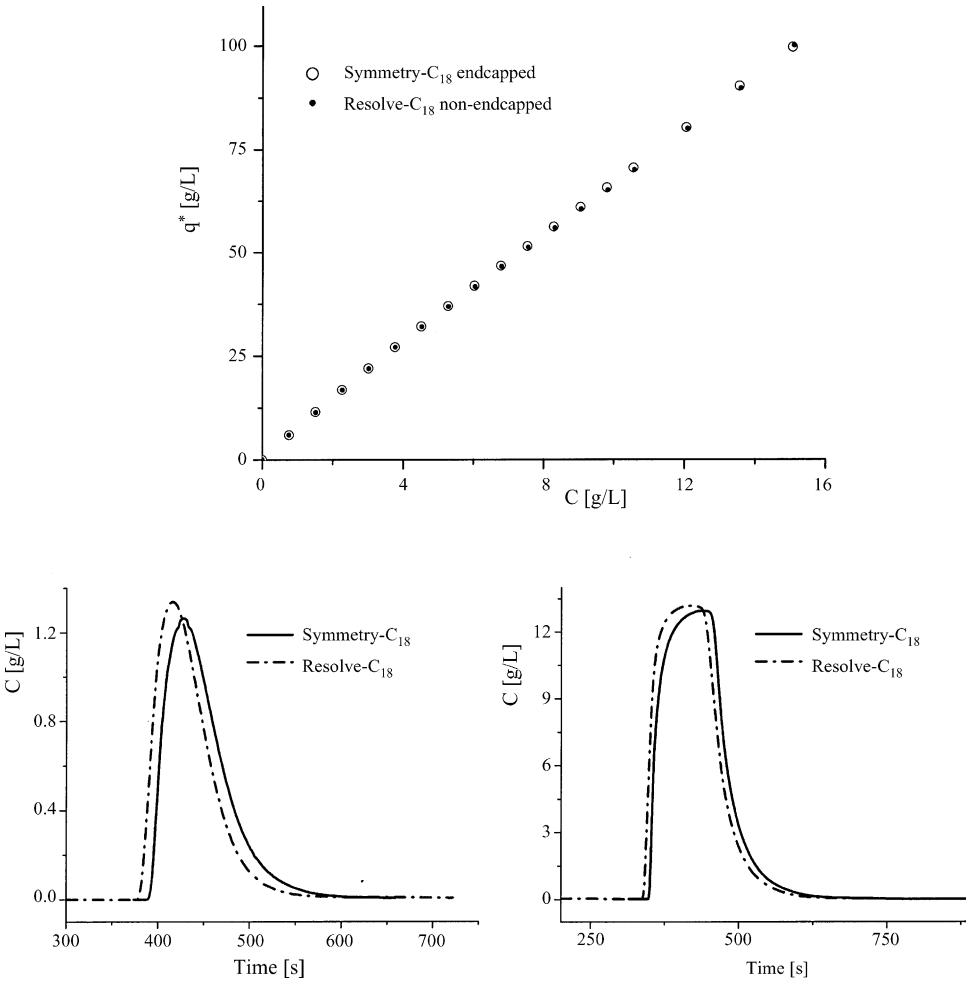

Fig. 1. (Top) Adsorption isotherm data of propylbenzoate on Resolve-C_{18} (small full circles) and Symmetry-C_{18} (large empty circles). Mobile phase methanol/water (65/35, v/v), $T = 296$ K. (Bottom) Experimental overloaded band profiles recorded at low (injection of a 1.5 g/L solution during 60 s) and high (injection of a 13.5 g/L solution during 90 s) column loadings.

Table 3
Comparison between the best isotherm parameters determined by the fitting of the frontal analysis data on the non-endcapped Resolve-C_{18} and the endcapped Symmetry-C_{18} columns

Solute							
Propylbenzoate		4-tert-Butylphenol		Caffeine			
MeOH (65)/H_2O (35)[a]		MeOH (60)/H_2O (40)[a]		MeOH (30)/H_2O (70)[a]		ACN (20)/H_2O (80)[a]	
BET[b]		Bi-Langmuir[b]		Quadri-Langmuir[b]	Tri-Langmuir[b]	Bi-Langmuir[b]	
Resolve[c]	Symmetry[c]	Resolve[c]	Symmetry[c]	Resolve[c]	Symmetry[c]	Resolve[c]	Symmetry[c]
Isotherm parameters							
$q_S = 98.7$, $b_S = 0.0804$, $b_L = 0.0236$	$q_S = 100.3$, $b_S = 0.0798$, $b_L = 0.0234$	$q_{S1} = 157.7$, $b_1 = 0.0058$	$q_{S1} = 128.9$, $b_1 = 0.0443$	$q_{S1} = 149.3$, $b_1 = 0.014$	$q_{S1} = 147.5$, $b_1 = 0.0136$	$q_{S1} = 113.0$, $b_1 = 0.0122$	$q_{S1} = 77.1$, $b_1 = 0.0124$
		$q_{S2} = 92.7$, $b_2 = 0.059$	$q_{S2} = 23.0$, $b_2 = 0.192$	$q_{S2} = 17.7$, $b_2 = 0.136$	$q_{S2} = 6.3$, $b_2 = 0.172$	$q_{S2} = 0.40$, $b_2 = 0.690$	$q_{S2} = 0.17$, $b_2 = 0.592$
				$q_{S3} = 1.2$, $b_3 = 1.3$	$q_{S3} = 0.004$, $b_3 = 104.2$		
				$q_{S4} = 0.02$, $b_4 = 62.2$			

The saturation capacities and the equilibrium constants are expressed in g/L and L/g, respectively.

[a] Mobile phase.
[b] Isotherm model.
[c] Column.

an inflection point and becomes convex downward at high concentrations. The BET isotherm model was found to be best to account for these adsorption data. The inflection point is located at about the same concentration on both columns. The agreement (not shown) between the experimental and the calculated band profiles is excellent in both cases, similar to the one shown previously [18–21]. Thus, the adsorption of propylbenzoate on Symmetry-C_{18} and on Resolve-C_{18} seems to be independent of the detailed chemistry of the adsorbent surface, at least in a mobile phase relatively rich in methanol.

The really surprising observation is that the two isotherms are nearly overlaid although the specific surface areas (200 m^2/g versus 346 m^2/g) and the bonding density (2.45 m^2/g versus 3.18 μmol/m^2) are much lower on Resolve-C_{18} than on Symmetry-C_{18}. However, the column hold-up volumes and the sums of the external and the internal pore volumes are very close (1.089 and 1.062 mL for the Resolve-C_{18} and the Symmetry-C_{18} columns, respectively). So, the column hold-up volume of the Resolve-C_{18} column is higher than that of the Symmetry-C_{18} column although the Resolve-C_{18} packing material has a much lower pore volume (0.5 mL/g versus 0.9 mL/g), although they have the same mesopore diameter, about 90 Å. Since the external porosities of different columns are very close, this means that the low bonding density of Resolve-C_{18} and its higher number of free surface silanols (which lead to a better wettability of the surface by the polar mobile phase) combine to allow the penetration of an equivalent volume of mobile phase inside the pores of the particles. The accessible hydrophobic surface area after bonding would then be the same for both adsorbents, explaining why the isotherm parameters measured are almost idendical

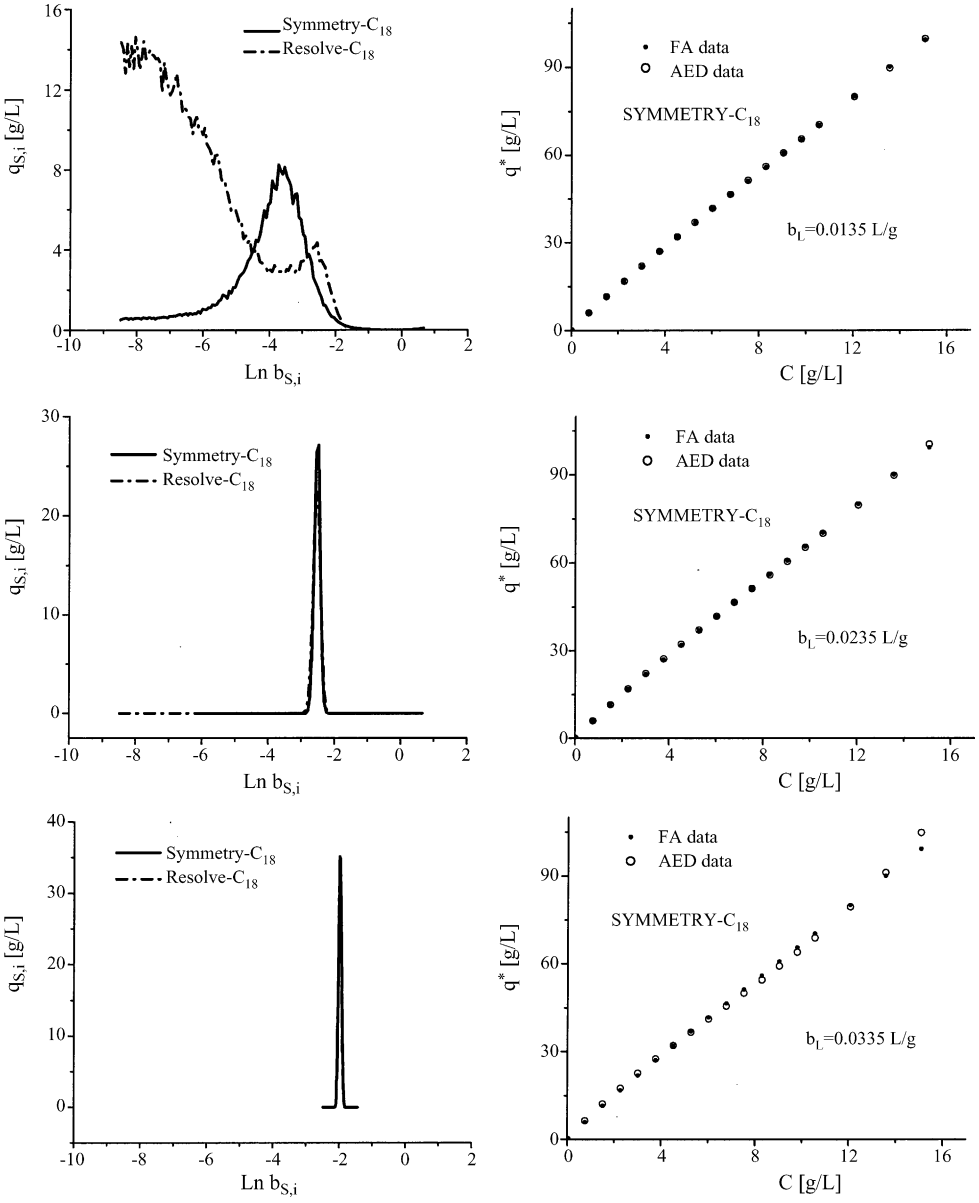

Fig. 2. (Left) Calculated AEDs of propylbenzoate on Symmetry-C_{18} and Resolve-C_{18} by the EM method. A local BET isotherm model was assumed in the calculations, with three different b_L parameters (0.0135, 0.0235 and 0.0335 L/g). (Right) Comparison between the experimental isotherm data (small full circles) and the calculated isotherm data derived fronm the AEDs (large empty circles).

(see Table 3). In addition, the favourable solvation of the C_{18} chains by a mobile phase rich in the organic modifier (60% in volume) certainly smooths out the effect of small differences in the bonding density so that the adsorption constants b_S measured are very close.

The AED of propylbenzoate was calculated directly from the FA adsorption data on both columns [15,16]. Because the experimental overall isotherm is not a simple convex upward isotherm, it would be inconsistent to use a Langmuir model for the local isotherm and the numerical calculation would fail. The local BET isotherm model was used instead. However, this model contains two independent equilibrium constants, b_S (the equilibrium constant between the surface and the first adsorbed layer) and b_L (the equilibrium constant between successive layers of adsorbate). In order to estimate the distribution of the saturation capacities, $q_{S,i}$ versus $b_{S,i}$, an assumption must be made for the value of b_L. Calculations were made with three different values, $b_L = 0.0235$ L/g (close from the best value found by the regression analysis of the isotherm data), a smaller, $b_L = 0.0135$ L/g, and a larger, 0.0335 L/g, value. The three sets of results are compared in Fig. 2 which compares also the isotherms derived directly from the experimental data (solid symbols) and those calculated by integration of the distribution function over the energy range (open symbols). For b_L values larger than 0.0235 L/g, the agreement is poor and the corresponding AED must be rejected. For b_L values lower than 0.0235 L/g, the AED does not converge after 1 million iterations toward a smoothed and well defined energy distribution and the result is poorly consistent with the overall isotherm. The unimodal energy distribution obtained with $b_L = 0.0235$ L/g is consistent with the isotherm results, with a single energy mode, centered around 0.0788 and 0.0803 L/g, for the Resolve-C_{18} and the Symmetry-C_{18} adsorbents, respectively, values that are in agreement with the FA regression parameters. Note that the two distributions are almost identical.

In conclusion, the end-capping of the stationary phase seems to have little or no effect on the adsorption behavior of propylbenzoate in RPLC when an aqueous mobile phase rich in methanol is used. The two columns exhibit nearly the same hold-up volume, the same saturation capacities and very similar equilibrium constants. The details of the surface chemistry are certainly hidden to the probe used and the formation of the multilayer system characteristic of the BET isotherm model takes place similarly in the mesopores of the two silica bonded mate-

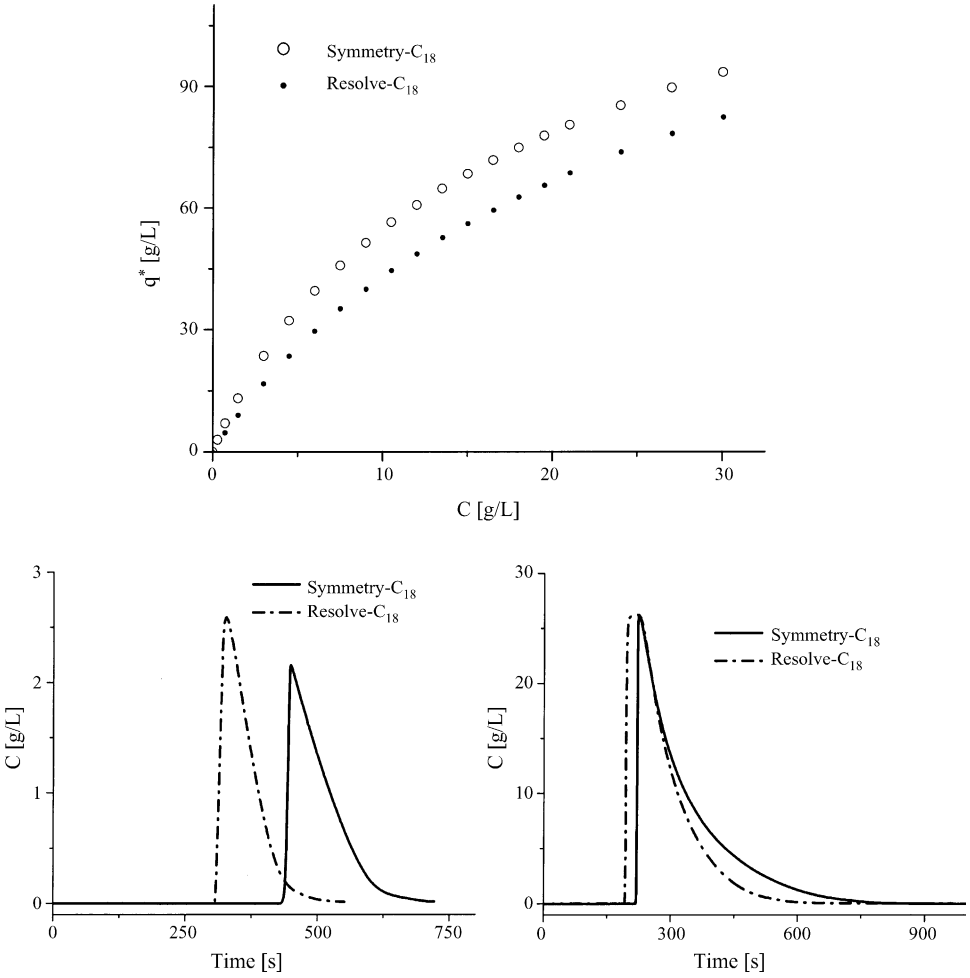

Fig. 3. (Top) Adsorption isotherm data of 4-*tert*-butylphenol on Resolve-C_{18} (small full circles) and Symmetry-C_{18} (large empty circles). Mobile phase methanol/water (60/30, v/v), $T = 296$ K. (Bottom) Experimental overloaded band profiles of 4-*tert*-butylphenol recorded at low (injection of a 3 g/L solution during 60 s) and high (injection of a 27 g/L solution during 90 s) column loadings. Note the larger retention on Symmetry-C_{18} while there is hardly any difference in Fig. 1.

rials used (which have the same average mesopore diameter of about 90 Å).

4.2. Adsorption of 4-tert-butylphenol on Resolve-C_{18} and Symmetry-C_{18} (MeOH/H_2O, 60/40, v/v)

We chose 4-*tert*-butylphenol for its sufficient retention factor and because phenols, being more polar than alkylbenzoates, exhibit adsorption isotherms on RPLC stationary phases that are strictly convex upward [18]. It has already been shown that the adsorption of phenol derivatives takes place only as a monolayer. The mobile phase used with 4-*tert*-butylphenol had a slightly higher water concentration than the one used with propylbenzoate (40% instead of 35% water, v/v). It was also shown in some previous reports that, with a mobile phase of very similar composition (38% water in volume), the isotherm is close to a simple Langmuir isotherm (i.e., it has a unimodal energy distribution and a quasi-linear Scatchard plot) [22].

The adsorption data measured by FA on the two adsorbents studied here are shown in Fig. 3. Although these two isotherms are quite similar, it is clear that the adsorption of 4-*tert*-butylphenol is stronger on the endcapped Symmetry-C_{18} column than on the non-endcapped Resolve-C_{18} column. The experimental Scatchard plots, shown in Fig. 4, are not strictly linear which means that the simple Langmuir isotherm model cannot exactly account for these adsorption data. This point was confirmed by the results of the calculation of the AEDs, also shown in Fig. 4. The two distributions are clearly bimodal. Accordingly, a bi-Langmuir isotherm model describes better the adsorption of 4-*tert*-butylphenol on the two adsorbents. The best parameters derived from the nonlinear regression are given in Table 3. The two equilibrium constants (b_1 and b_2) are much larger on Symmetry-C_{18} than on Resolve-C_{18} (nine and three times, respectively). On the other hand, the saturation capacities are larger on Resolve-C_{18}, particularly that of the high-energy sites. This latter represents 37% of the total saturation capacity of the non-endcapped adsorbent but only 15% of that of the endcapped adsorbent. These values of the isotherm parameters illustrate the higher degree of surface heterogeneity of the non-endcapped material regarding the adsorption of 4-*tert*-butylphenol. Fig. 5 compares the band profiles obtained for 4-*tert*-butylphenol at moderate and high loading factors on the two columns. The agreement observed confirms the validity of the isotherm model.

Despite the similar content of methanol in the mobile phase used for the measurements of their adsorption data (60%, v/v,

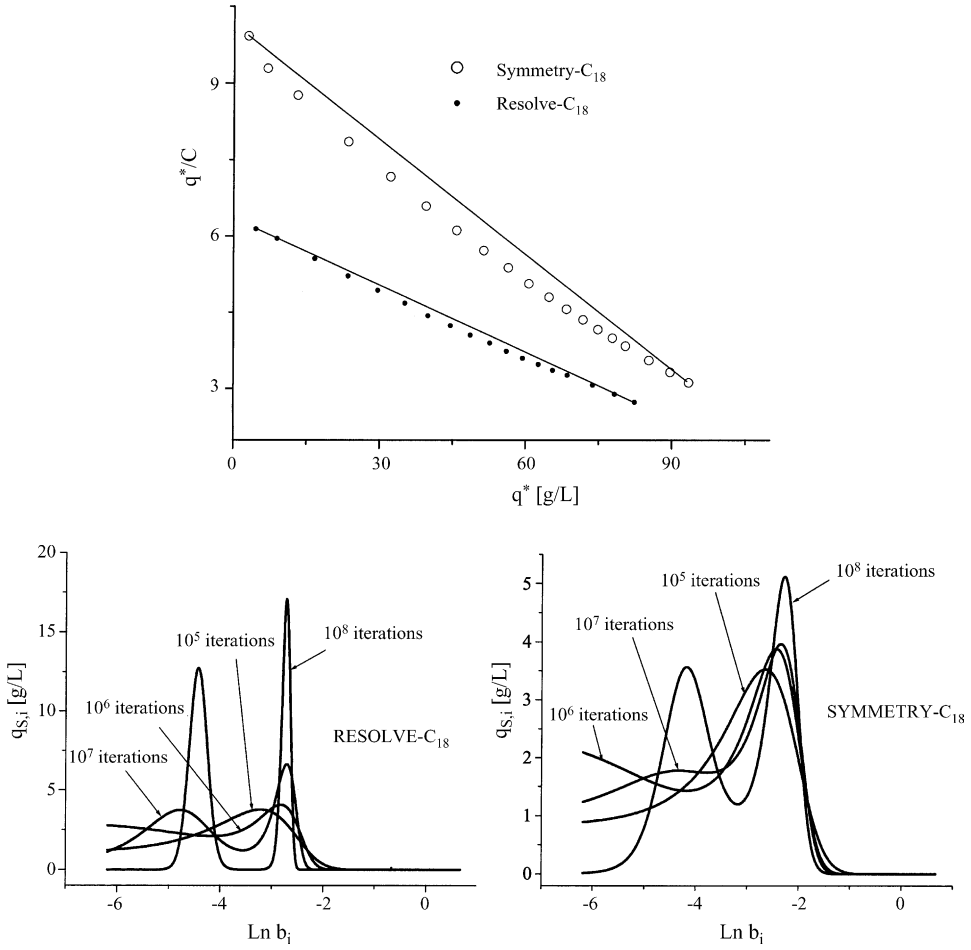

Fig. 4. (Top) Scatchard representation (plot of q/C vs. q) of the adsorption data of 4-*tert*-butylphenol on the Symmetry-C_{18} and Resolve-C_{18} adsorbents. Note that the plots are not straight lines suggesting a heterogeneous surface. (Bottom) Calculated AEDs of 4-*tert*-butylphenol on Symmetry-C_{18} and Resolve-C_{18} by the EM method. A local Langmuir isotherm model was assumed in the calculations. Note a bimodal distribution in both cases.

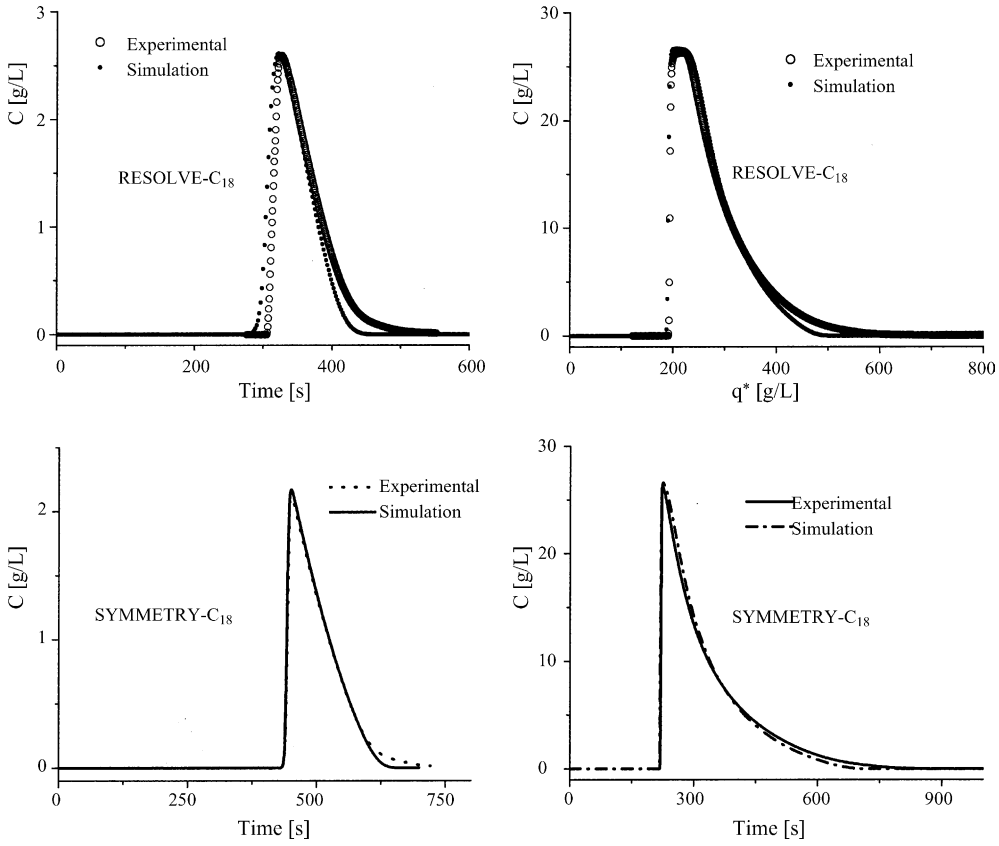

Fig. 5. Comparison between experimental and calculated (using the ED model of chromatography and the best Bi-Langmuir isotherm) overloaded band profiles of 4-*tert*-butylphenol recorded at low (injection of a 3 g/L solution during 60 s) and high (injection of a 27 g/L solution during 90 s) column loadings.

for 4-*tert*-butylphenol versus 65% for propylbenzoate), the adsorption behavior of these two compounds is clearly different. However, for either one the behavior is very close on the endcapped and the non-endcapped adsorbents. The reason for the difference in adsorption behavior of the two compounds is that the molecules of propylbenzoate tend to associate around the alkyl ligands bound to silica and do not probe the very details of the adsorbent surface. Their adsorption is likely to be mostly controlled by the thermodynamics in the liquid phase, e.g., by the mobile phase composition. As expected from the higher bonding density and the higher hydrophobicity of the C_{18}-bonded surface of Symmetry-C_{18}, 4-*tert*-butylphenol is more retained on this adsorbent although it has relatively fewer high-energy sites than Resolve-C_{18}. The endcapping limits the degree of surface heterogeneity which arises from the coexistence of patches of high density of C_{18} alkyl chains and patches of low chain density, where the density of unreacted silanols is higher.

The difference between the adsorption behaviors of propylbenzoate and 4-*tert*-butylphenol could be due to the difference between the molecular interactions of the silanol groups and the ester or the hydroxyl group. The hydrogen bond basicity of propylbenzoate (e.g., its propensity to bond to the hydrogen of a hydroxyl group) is different from zero [23]. The solute hydrogen bond basicity descriptor $\sum \beta_2^H$ of diethyl phthalate is 0.88 (thus, that of propylbenzoate is 0.44) and that of 4-ethylphenol is 0.36. Accordingly, the affinities of propylbenzoate and phenol for the silanol group are comparable. However, previous experiments [10] showed that phenol does not interact with the silanol groups of the non-endcapped Resolve-C_{18}; hence, neither does propylbenzoate. In contrast to propylbenzoate, 4-*tert*-butylphenol forms an adsorbed monolayer and is more sensitive to the local structure of the stationary phase (its heterogeneity, chain density, etc.). Its saturation capacities are much larger (1660 and 1010 mmol/L on Resolve and Symmetry, respectively) than those measured for propylbenzoate (610 mmol/L only on either adsorbent). The alternative interpretation suggested above is inconsistent with these facts.

4.3. Adsorption of caffeine on Resolve-C_{18} and Symmetry-C_{18} (MeOH/H_2O, 30/70, v/v)

Caffeine being quite soluble in the mobile phase, the methanol concentration in the mobile phase had to be considerably decreased, from 60 to 30%, in order to achieve the sufficient retention that is required in order to make accurate measurements. We know, however, that the conformation of the bonded C_{18} alkyl chains is affected by mobile phase composition. The solvation strength of the mobile phase decreases with increasing water content. The chains tend to collapse, which increases the pore volume, a result consistent with the larger total column porosity measured with this new mobile phase (see Table 2). We have observed previously [10] that the surface of Resolve-C_{18} is much more heterogeneous than that of endcapped Symmetry-

C_{18}. We identified four types of adsorption sites having a different adsorption behavior toward caffeine on the non-endcapped material but only two different types of sites on the endcapped column. These three high-energy types of sites on Resolve-C_{18} (and the high-energy sites on Symmetry) were attributed to as many types of hydrophobic cages embedded within the C_{18}-bonded layer, none to any strong polar interactions.

The caffeine adsorption data measured by FA on the two adsorbents are shown in Fig. 6. The isotherms are convex upward on both columns. Surprisingly, the amount adsorbed on the stationary phase at a given mobile phase concentration is now higher on Resolve-C_{18} than on Symmetry-C_{18}, in contrast to what was observed for 4-*tert*-butylphenol (see Fig. 3). Such a reversal of the adsorption behavior is related in part to the consequences on the conformation of the bonded ligands of the change of the mobile phase composition (i.e., the large decrease of the methanol content). The relative position of the two band profiles in Fig. 6 confirms this point. The retention of caffeine at moderate loading factor (left graph) is higher on Resolve-C_{18} than on Symmetry-C_{18} because the high-energy sites are stronger but the bands are very close at high loadings because the behaviors of the low-energy sites on both adsorbents are quite similar (see Table 3).

In a previous study [10], the heterogeneity of Resolve-C_{18} toward the adsorption of caffeine from a 25:75 (v/v) methanol:water solution was characterized by a four modes AED. The AEDs obtained in this similar case (30:70 methanol:water solution) are shown in Fig. 7. These AEDs are quadrimodal on Resolve-C_{18} and trimodal on Symmetry-C_{18}. The smaller the saturation capacities, the higher the associated equilibrium constant, which means that the different types of sites have individual contributions to the retention factor (i.e., the product $b_i q_{s,i}$) that are all comparable (see Table 3). More specifically, the saturation capacity of the highest energy mode is very small on both adsorbents (about 0.02 and 0.004 g/L) and represents only 0.01 and 0.003% of the total saturation capacities. For this reason, it is difficult to give a clear physical interpretation of the nature of these sites. It is possible that the high-energy modes are due to some numerical artefacts generated by the EM program. However, other adsorption studies on non-endcapped materials have demonstrated the physical reality of the fourth type of adsorption sites [24]. We note that the low-energy modes on the two adsorbents have the same adsorption constant, hence must correspond to the same interaction, probably that with solvated alkyl chains. The differences between the columns are explained by the different properties of the high-energy sites

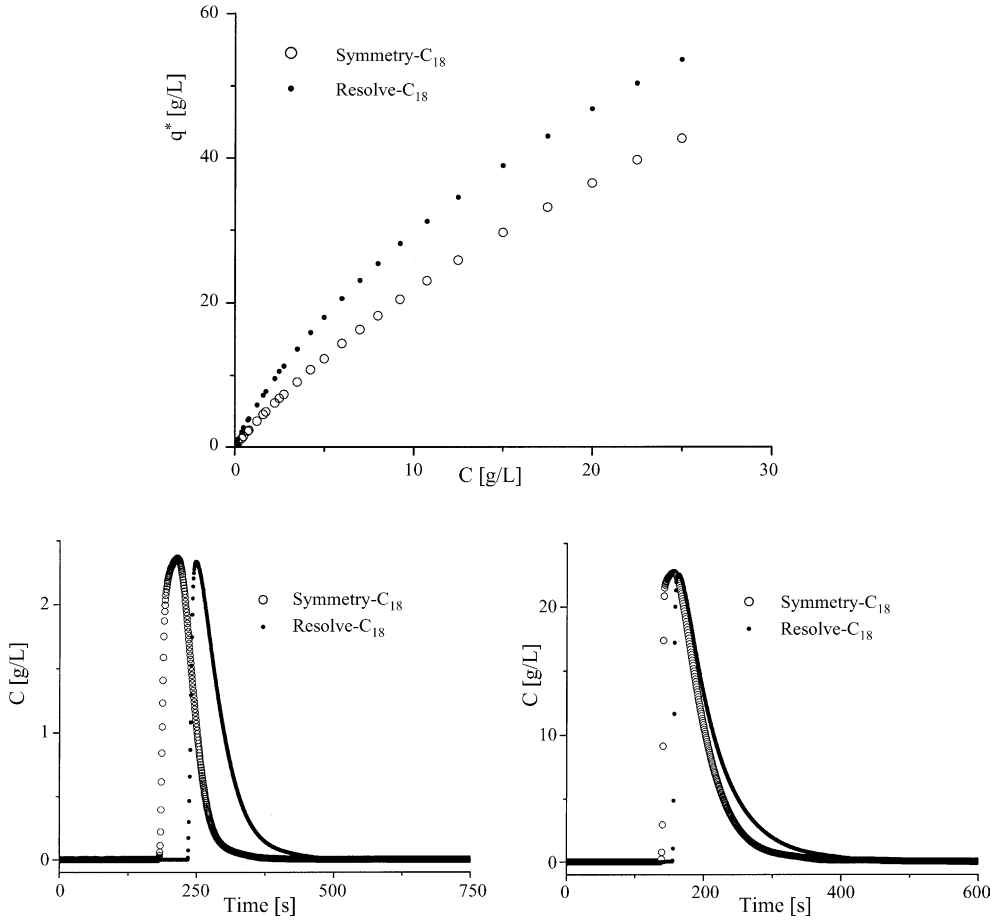

Fig. 6. (Top) Adsorption isotherm data of caffeine on Resolve-C_{18} (small full circles) and Symmetry-C_{18} (large empty circles). Mobile phase methanol/water (60/40, v/v), $T = 296$ K. (Bottom) Experimental overloaded band profiles of caffeine recorded at low (injection of a 2.5 g/L solution during 60 s) and high (injection of a 25 g/L solution during 60 s) column loadings. Note the larger retention on Resolve-C_{18} by comparison to Fig. 3. Methanol:water mobile phase (30/70, v/v).

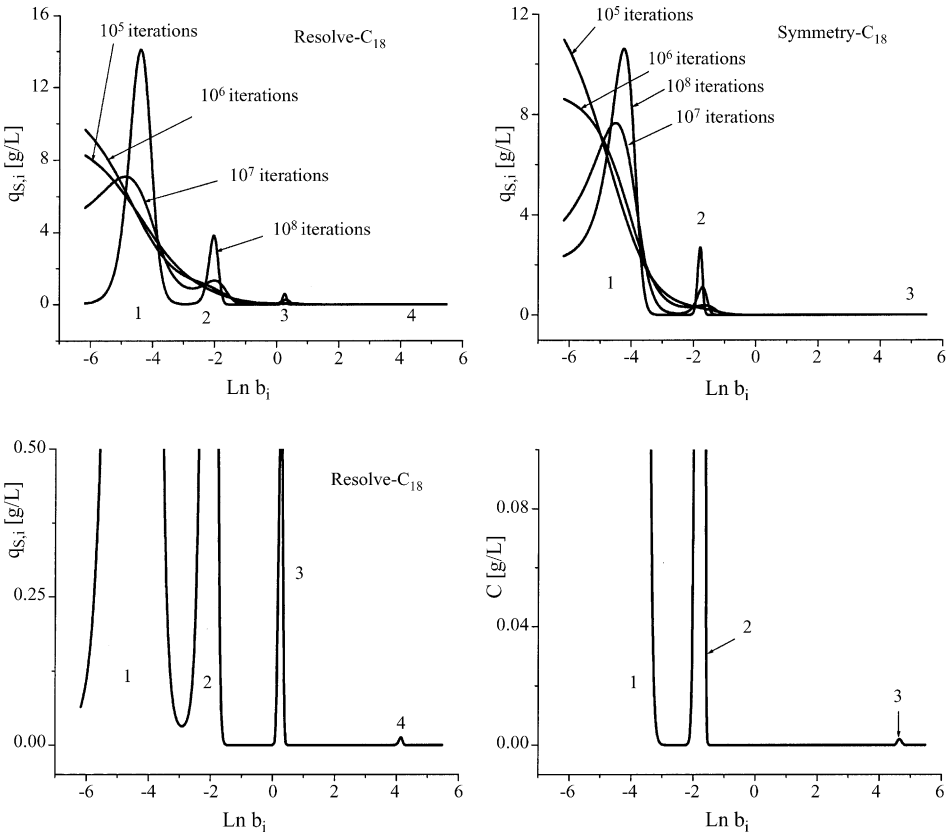

Fig. 7. Calculated AEDs of caffeine on Resolve-C_{18} and Symmetry-C_{18} by the EM method. A local Langmuir isotherm model was assumed in the calculations. Methanol:water mobile phase (30/70, v/v). Note the multi-modal distributions (three and four modes) showing that the surface heterogeneity is high with water-rich mobile phases.

which certainly correspond to large hydrophobic cages within the C_{18}-bonded layer. Fig. 8 shows the very good agreement between the experimental and the calculated band profiles derived from the ED model, using the quadri- (on Resolve) and the tri- (on Symmetry) Langmuir isotherm models (parameters in Table 3). The higher degree of surface heterogeneity of Resolve-C_{18} is certainly related to the absence of endcapping of this silica surface. It is enhanced by the low methanol concentration in the mobile phase. The "endcapping free" spaces become available sites for the adsorption of caffeine molecules but they probably become hidden at high methanol concentrations when the C_{18} alkyl chains unfold and their layer swells.

4.4. Adsorption of caffeine on Resolve-C_{18} and Symmetry-C_{18} (ACN/H_2O, 20/80, v/v)

Finally, we compared the adsorption behavior of caffeine on the endcapped Symmetry-C_{18} and the nonendcapped Resolve-C_{18} adsorbents when acetonitrile is used as the organic modifier of the mobile phase instead of methanol. Acetonitrile is known to be the stronger organic modifier. The substitution of the former to the latter leads to an important decrease of the retention. Two reasons are commonly advanced to explain this observation. (1) The solubility of the analytes increases, hence their retention decreases in RPLC; and (2) acetonitrile adsorbs on the adsorbent (the retention factor of acetonitrile in pure water is much larger than unity) and it compete with the analyte for the adsorption.

The adsorption isotherm data acquired on the two columns are shown in Fig. 9. The results are qualitatively similar to those observed with methanol (Fig. 6) but, for a given mobile phase concentration, the amount of caffeine adsorbed at equilibrium is smaller, about four-fold, in spite of the large decrease in the concentration of organic modifier in the mobile phase. The AEDs are shown in Fig. 10. They are obviously bimodal (in agreement with the curved Scatchard plot shown in Fig. 9) and the isotherms on both adsorbents are now Bi-Langmuir. The best coefficients of the Bi-Langmuir isotherms are given in Table 3. The saturation capacities are close to those measured for propylbenzoate with a 65% methanol concentration in the mobile phase (around 100 g/L). They are significantly lower than those found at low methanol concentrations ($q_S \geq 150$ g/L, Table 3). In contrast with the result obtained with methanol, the concentration of the high-energy sites is rather small, less than 0.4% of the total monolayer capacity.

Note that the adsorption isotherm of caffeine would probably not follow strictly a convex upward isotherm model (e.g., a Bi-Langmuir isotherm model) if the largest concentration of caffeine applied was increased from 40 to 80 g/L. Thus, the adsorption isotherm of caffeine on Discovery-C_{18} is best described by a Langmuir-BET model, because adsorbate-adsorbate interactions take place at high concentrations in the thick layer of acetonitrile adsorbed at the interface between the bulk mobile phase and the bonded chains [25].

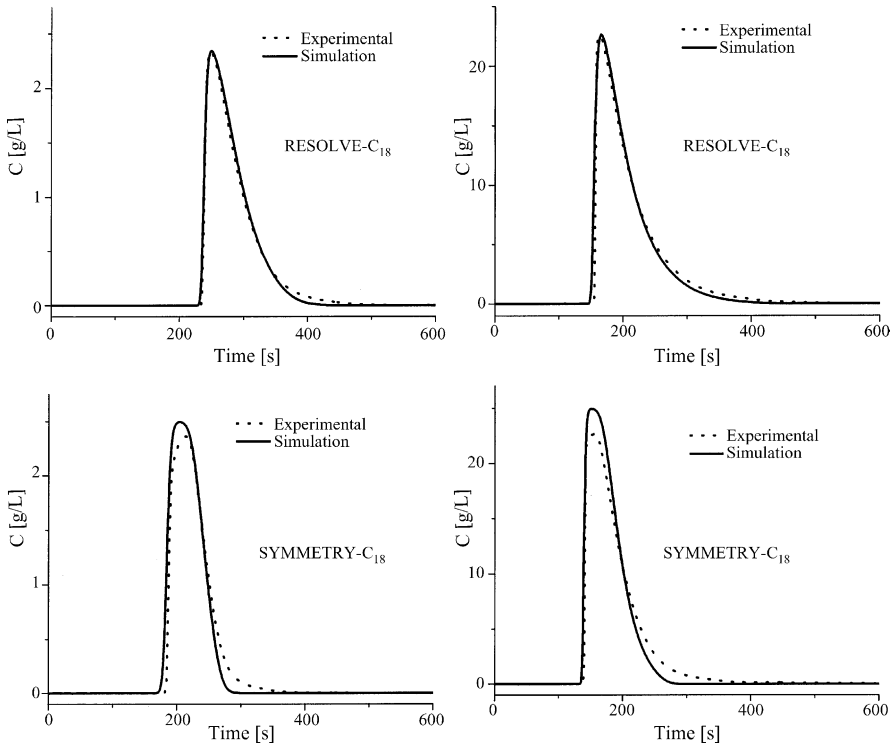

Fig. 8. Experimental and calculated (using the ED model of chromatography and the best Bi-Langmuir isotherm) overloaded band profiles of caffeine recorded at low (injection of a 2.5 g/L solution during 60 s) and high (injection of a 25 g/L solution during 60 s) column loadings.

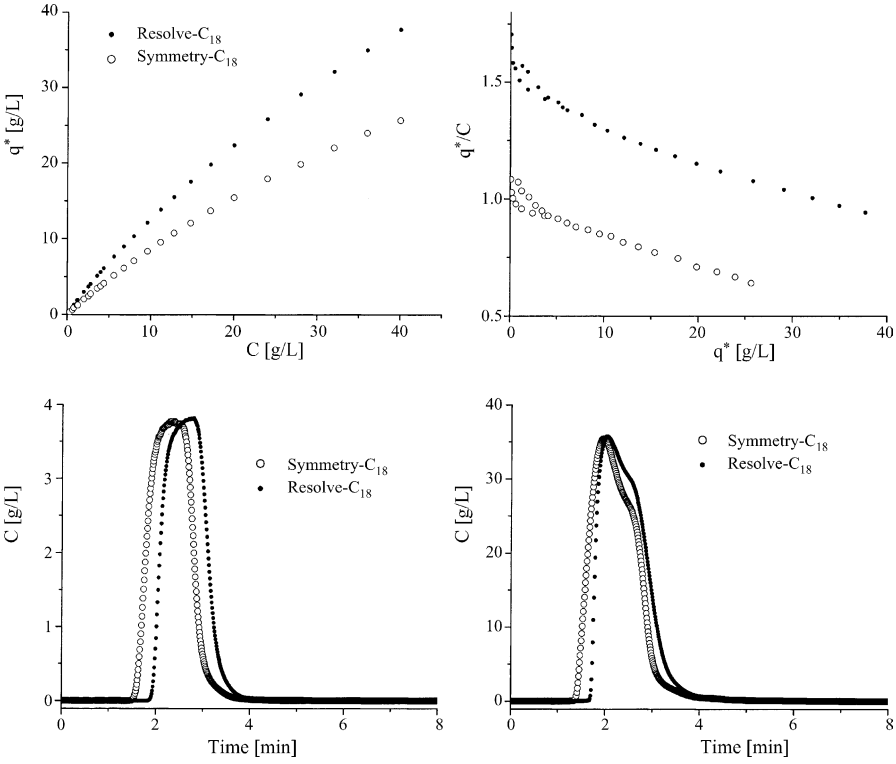

Fig. 9. (Upper left) Adsorption isotherm data of caffeine on Resolve-C_{18} (small full circles) and Symmetry-C_{18} (large empty circles). Mobile phase acetonitrile/water (20/80, v/v), $T = 296$ K. (Upper right) Scatchard plot of the adsorption data in the upper left graph. Note the quasi linear plot except at low values of q^*. (Bottom) Experimental overloaded band profiles of caffeine recorded at low (injection of a 2.5 g/L solution during 60 s) and high (injection of a 25 g/L solution during 60 s) column loadings. Acetonitrile:water mobile phase (20/80, v/v).

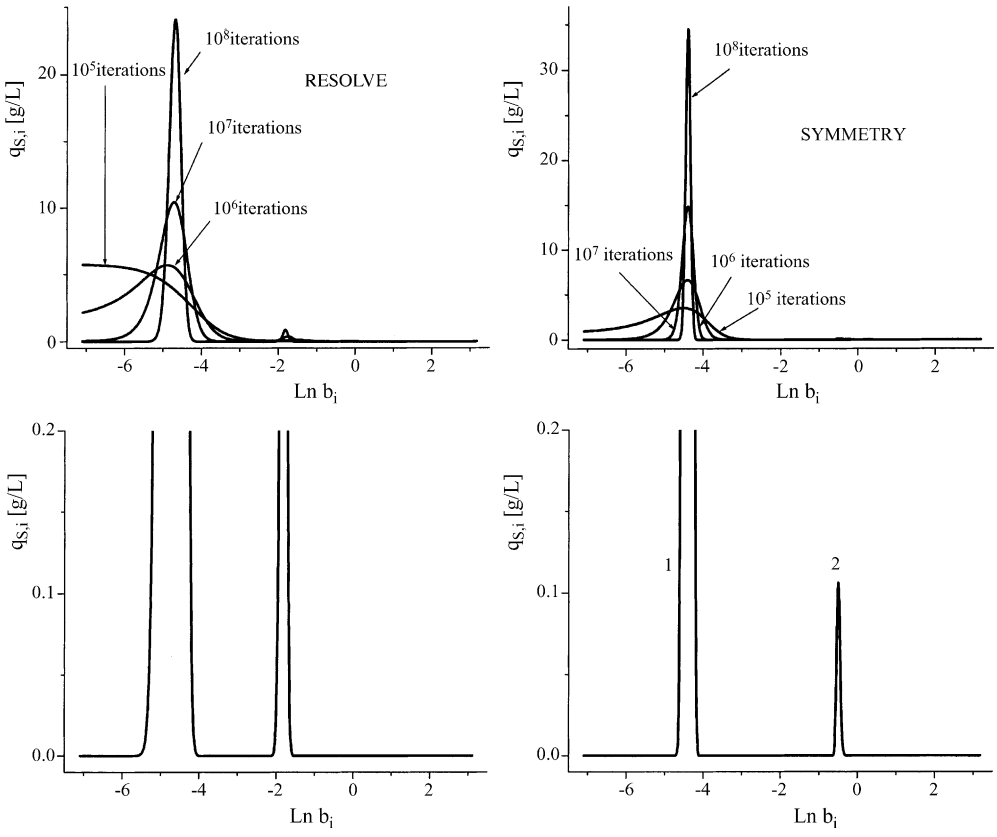

Fig. 10. Calculated AEDs of caffeine on Resolve-C_{18} and Symmetry-C_{18} by the EM method. A local Langmuir isotherm model was assumed in the calculations. Acetonitrile:water mobile phase (20/80, v/v). Note the simple bimodal distributions showing a lesser degree of surface heterogeneity by comparison to Fig. 7.

In other words, despite a retention comparable to that observed with 30% methanol in the mobile phase, the presence of 20% acetonitrile in the mobile phase drastically reduces the surface heterogeneity of both Resolve-C_{18} and Symmetry-C_{18}. These adsorbents now behave almost as if they had homogeneous surfaces. We can explain this result by the highest affinity of acetonitrile for the C_{18}-bonded chaims. It has long been known that acetonitrile adsorbs more strongly on C_{18}-bonded phases than methanol [26,27]. The adsorption of acetonitrile from water was considered as the formation of a multilayer adsorbed phase that covers and solvates the apolar surface of the adsorbent, while methanol forms simply a monolayer. The acetonitrile adsorbed layer (which may count up to four of five molecular layers, stacked on top of each other) shields the structure heterogeneity of the C_{18}-bonded layer. The retention mechanism of the solute could then be described as the superimposition of two processes [25]. (1) The analyte partitions between the liquid phase (acetonitrile:water mixture) and the multilayer adsorbed phase (quasi pure acetonitrile); and (2) the analyte adsorbs from the pure acetonitrile layer against the surface of the bonded phase. This second process could explain why the retention of caffeine is so weak compared to that of phenol, the distribution coefficient between adsorption and solution in the pure acetonitrile is small.

The differences in the retention mechanisms from methanol and acetonitrile solutions are illustrated by the unusual shape of the desorption front of high concentration bands shown in Fig. 9. Similar observations were made for the shape of the breakthrough curves [25]. On either adsorbent, high concentration bands always exhibit a shoulder on their desorption front. The origin of this phenomenon is probably related to the different desorption rates, one fast at the interface between the bulk liquid phase and the adsorbed layer of pure acetonitrile, and one slow at the interface between the bonded phase and the acetonitrile multilayer phase.

5. Conclusion

Our results demonstrate that there are some moderate differences between the adsorption isotherm behavior of small-molecule compounds on a non-endcapped adsorbent (Resolve-C_{18}) and on an endcapped one (Symmetry-C_{18}). The endcapping is currently applied to prevent excessive peak tailing of basic compounds due to their interactions with the acidic unreacted silanol groups. Compounds that are not basic or are poorly so (e.g., propylbenzoate, 4-*tert*-butylphenol, and caffeine) are not expected to experience a great change in their adsorption behavior. Our results show that the mobile phase composition (i.e., the nature and the concentration of the organic modifier) plays a crucial role to distinguish between the adsorption behavior on a non-endcapped and an endcapped adsorbent. At high organic modifier concentrations, the C_{18}-bonded alkyl chains are more solvated and no or few differences are observed. The endcapping process does not re-

sult in an adsorption mechanisnm of non-basic compounds that is different from the mechanism on non-endcapped adsorbents because the C_{18} chains are unfolded and shield the silanol groups.

On the other hand, it is possible easily to distinguish between the behavior of an endcapped and a non-endcapped adsorbent by decreasing the organic content of the mobile phase. The isotherm models that best account for the adsorption data are often quite different on the two types of adsorbents and the degree of surface heterogeneity of the non-endcapped adsorbent is systematically higher. As previously reported [10], non-endcapped adsorbents have a more heterogeneous surface in water-rich mobile phases. The C_{18}-chains tends to collapse on each other forming hydrophobic cages in the process, in regions where unreacted silanols are present. This phenomenon seems less frequent and important with endcapped adsorbents. Usually, endcapped adsorbents exhibit one or two fewer degrees of heterogeneity than non- endcapped adsorbents. Finally, the nature of the organic modifier plays also a major role in the differentiation of endcapped and non-endcapped. Using acetonitrile (or a stronger modifier) instead of methanol levels out the differences between the two types of adsorbent. The origin of this phenomenon seems to remain the same, the higher degree of solvation of the C_{18}-bonded chains by the mobile phase. As demonstrated elsewhere, the adsorption mechanism of neutral analytes on C_{18}-bonded surfaces is different with methanol and acetonitrile [25]. The analyte forms an adsorbed monolayer in the presence of methanol. At sufficiently high concentrations, it forms a multilayer system, dissolved in the thick (ca. 14 Å) layer of acetonitrile adsorbed as a four molecular layer system on the surface of C_{18} RPLC columns.

Accordingly, the interpretation of retention data in RPLC should be made cautiously when aqueous mobile phases rich in water are used, particularly with non-endcapped adsorbents. The access of the molecules of analyte to the unendcapped zones of the bonded silica surface becomes possible and this changes considerably the adsorption behavior compared to the one on endcapped adsorbents. The heterogeneity of the reversed-phase materials increases and additionnal high-energy sites appear that have an important effect at low concentrations.

Acknowledgments

This work was supported in part by grant CHE-02-44693 of the National Science Foundation, by Grant DE-FG05-88-ER-13869 of the US Department of Energy, and by the cooperative agreement between the University of Tennessee and the Oak Ridge National Laboratory. We thank Uwe Neue and Marianna Kele (Waters Corporation, Milford, MA, USA) for the generous gift of the columns used in this work and for fruitful and creative discussions.

References

[1] J. Nawrocki, J. Chromatogr. A 779 (1997) 29.
[2] S.D. Rogers, J.G. Dorsey, J. Chromatogr. A 892 (2000) 57.
[3] G.B. Cox, J. Chromatogr. A 656 (1993) 353.
[4] U.D. Neue, A. Mendez, K. Van tran, J. Chromatogr. A 779 (1997) 29.
[5] F. Gritti, G. Guiochon, J. Chromatogr. A 1038 (2004) 53.
[6] F. Gritti, G. Guiochon, J. Chromatogr. A 1041 (2004) 63.
[7] F. Gritti, G. Guiochon, J. Chromatogr. A 1033 (2004) 43.
[8] F. Gritti, G. Guiochon, J. Chromatogr. A 1033 (2004) 57.
[9] F. Gritti, G. Guiochon, Anal. Chem. 76 (2004) 4779.
[10] F. Gritti, G. Guiochon, J. Chromatogr. A 1028 (2004) 75.
[11] G. Guiochon, S.G. Shirazi, A.M. Katti, Fundamentals of Preparative and Nonlinear Chromatography, Academic Press, Boston, MA, 1994.
[12] G. Guiochon, J. Chromatogr. A 965 (2002) 129.
[13] G. Schay, G. Szekely, Acta Chem. Hung. 5 (1954) 167.
[14] D.H. James, C.S.G. Phillips, J. Chem. Soc. (1954) 1066.
[15] F. Gritti, G. Guiochon, J. Chromatogr. A 1003 (2003) 43.
[16] B.J. Stanley, S.E. Bialkowski, D.B. Marshall, Anal. Chem. 659 (1994) 27.
[17] M. Jaroniec, R. Madey, Physical Adsorption on Heterogeneous Solids, Elsevier, Amsterdam, 1988.
[18] F. Gritti, W. Piątkowski, G. Guiochon, J. Chromatogr. A 978 (2002) 81.
[19] F. Gritti, W. Piątkowski, G. Guiochon, J. Chromatogr. A 983 (2003) 51.
[20] W. Piątkowski, F. Gritti, K. Kaczmarski, G. Guiochon, J. Chromatogr. A 989 (2003) 207.
[21] W. Piątkowski, D. Antos, F. Gritti, G. Guiochon, J. Chromatogr. A 1003 (2003) 73.
[22] F. Gritti, G. Guiochon, J. Chromatogr. A 1008 (2003) 23.
[23] M.H. Abraham, J. Andonian-Haftvan, G.S. Whiting, A. Leo, R.S. Taft, J. Chem. Soc., Perkin Trans. 2 (1994) 1777.
[24] F. Gritti, G. Guiochon, Anal. Chem. 77 (2005) 1020.
[25] F. Gritti, G. Guiochon, Anal. Chem. 77 (2005) 4257.
[26] I. Rustamov, T. Farcas, F. Ahmed, F. Chan, R. Lobrutto, H.M. McNair, Y.V. Kazakevich, J. Chromatogr. A 913 (2001) 49.
[27] Y.V. Kazakevich, R. Lobrutto, F. Chan, T. Patel, J. Chromatogr. A 913 (2001) 75.